INL/CON-11-22221
PREPRINT

Long-Term Performance of Solid Oxide Stacks with Electrode-Supported Cells Operating in the Steam Electrolysis Mode

IMECE 2011

J. E. O'Brien
R. C. O'Brien
X. Zhang
G. G. Tao
B. J. Butler

November 2011

The INL is a
U.S. Department of Energy
National Laboratory
operated by
Battelle Energy Alliance

Proceedings of the ASME 2011 International Mechanical Engineering Congress & Exposition
IMECE2011
November 11-17, 2011, Denver, Colorado, USA

IMECE2011-62581

LONG-TERM PERFORMANCE OF SOLID OXIDE STACKS WITH ELECTRODE-SUPPORTED CELLS OPERATING IN THE STEAM ELECTROLYSIS MODE

J. E. O'Brien
Idaho National Laboratory
Idaho Falls, Idaho, USA

R. C. O'Brien
Center for Space Nuclear Research
Idaho Falls, Idaho, USA

X. Zhang
Idaho National Laboratory
Idaho Falls, Idaho, USA

G. G. Tao
Materials and Systems Research, Inc.
Salt Lake City, Utah, USA

B. J. Butler
Materials and Systems Research, Inc.
Salt Lake City, Utah, USA

ABSTRACT

Performance characterization and durability testing have been completed on two five-cell high-temperature electrolysis stacks constructed with advanced cell and stack technologies. The solid oxide cells incorporate a negative-electrode-supported multi-layer design with nickel-zirconia cermet negative electrodes, thin-film yttria-stabilized zirconia electrolytes, and multi-layer lanthanum ferrite-based positive electrodes. The per-cell active area is 100 cm^2. The stack is internally manifolded with compliant seals. Treated metallic interconnects with integral flow channels separate the cells and electrode gases. Stack compression is accomplished by means of a custom spring-loaded test fixture. Initial stack performance characterization was determined through a series of DC potential sweeps in both fuel cell and electrolysis modes of operation. Results of these sweeps indicated very good initial performance, with area-specific resistance values less than 0.5 $\Omega.cm^2$. Long-term durability testing was performed with a test duration of 1000 hours. Overall performance degradation was less than 10% over the 1000-hour period. Final stack performance characterization was again determined by a series of DC potential sweeps at the same flow conditions as the initial sweeps in both electrolysis and fuel cell modes of operation. A final sweep in the fuel cell mode indicated a power density of 0.356 W/cm^2, with average per-cell voltage of 0.71 V at a current of 50 A.

INTRODUCTION

There is a growing interest in the development of large-scale non-fossil hydrogen production technologies. This interest is driven by the near-term demand for hydrogen for refining of increasingly low-quality petroleum resources, the expected intermediate-term demand for carbon-neutral synthetic fuels, and the potential long-term demand for hydrogen as an environmentally benign direct transportation fuel [1 - 3]. Additional important non-transportation markets for large-scale hydrogen production include ammonia production and (potentially) carbon-free steel production [4]. At present, hydrogen production in North America is based almost exclusively on steam reforming of methane. From a long-term perspective, methane reforming may not be sustainable for large-scale hydrogen production since natural gas is a non-renewable resource that exhibits large volatility in price and since methane reforming and other fossil-fuel conversion processes emit large quantities of greenhouse gases to the environment [5]. Non-fossil carbon-free options for hydrogen production include conventional water electrolysis coupled to either renewable (e.g., wind) energy sources or nuclear energy. The renewable-hydrogen option may be viable as a supplementary source, but would be very expensive as a large-scale stand-alone option [6, 7]. Conventional electrolysis coupled to nuclear base-load power can approach economical viability when combined with off-peak power, but the capital cost is high [8]. To achieve higher overall hydrogen production efficiencies, high-temperature thermochemical [9] or electrolytic [10] processes can be used. The required high temperature process heat can be based on concentrated solar energy [11] or on nuclear energy from advanced high-temperature reactors [12]. From 2003 – 2009, development and demonstration of advanced nuclear hydrogen technologies were supported by the US Department of Energy under the Nuclear Hydrogen Initiative (NHI) [13]. High temperature steam electrolysis was demonstrated as a feasible technology under this program, which included a 15 kW HTE technology demonstration, achieving a hydrogen production rate in excess

of 5000 NL/hr [14]. During 2009, the NHI program sponsored a technology down-selection activity by which an independent review team recommended HTE as the most appropriate advanced nuclear hydrogen production technology for near-term deployment [15]. HTE research is currently supported by the DOE Office of Nuclear Energy under the Next Generation Nuclear Plant (NGNP) Program [12].

The ultimate cost of hydrogen production by any technology is dependent on both capital and operating costs. In order to achieve competitive capital costs, HTE cells and stacks must exhibit both high performance and low degradation rates. Although HTE has been successfully demonstrated, our experience to date has indicated that solid oxide electrolysis cell (SOEC) and stack degradation must be improved prior to deployment of HTE as a viable cost-competitive technology. Consequently, the current focus of our research is to identify the mechanisms responsible for accelerated degradation in the electrolysis mode. Once these mechanisms are fully understood and ranked in terms of importance, effective mitigation strategies can be developed. Possible degradation mechanisms include transport of impurities leading to electrode poisoning and deactivation [16], coarsening of electrodes [17], loss of electrolyte ionic conductivity [18], depletion of oxygen vacancies in mixed conducting electrodes [19, 20], and electrode delamination [21].

Anode-supported cells represent the state of the art for solid oxide fuel cells. In the electrolysis mode, the nickel cermet electrode becomes the cathode. Depending on the material set, operation of these cells in the electrolysis mode can result in accelerated degradation and delamination of the oxygen electrode. The objective of the High Temperature Steam Electrolysis research program at the Idaho National Laboratory is to support development of SOECs and stacks that can achieve both high initial performance and low degradation rates. Performance degradation of 0.5%/khr or lower is required for commercial viability.

The cells and stacks used for these tests were supplied by Materials and Systems Research (MSRI), Inc. The cells were fabricated using MSRI's state-of-the-art fabrication processes specifically for operation in the steam electrolysis mode. In order to minimize possible cell variation among batches, a large batch of cells using MSRI's advanced SOEC material set were produced. Ten cells were randomly selected from a pool of twenty cells and were assembled into two identical 5-cell stacks. In addition, all non-cell repeat units for the construction of the stacks were identical, including dry contact aids, seal gaskets and interconnects. One stack was delivered to INL on January 10, 2011 for independent testing, with MSRI's staff present on-site providing assistance in the stack installation and testing. The second identical stack was tested at MSRI. Testing included initial performance evaluation in both the fuel cell and electrolysis modes of operation, followed by long-term (1000 hrs) durability testing. Results of tests performed at both locations are included in this paper.

NOMENCLATURE

ASR	=	Area-Specific Resistance, Ω cm^2
DAC	=	Digital to Analogue Converter
DOE	=	U.S. Department of Energy
HTSE	=	High Temperature Steam Electrolysis
INL	=	Idaho National Laboratory
NASA	=	National Aeronautics and Space Administration
NGNP	=	Next Generation Nuclear Plant
OCV	=	Open Cell Voltage
P&ID	=	Piping & Instrumentation Diagram
SOEC	=	Solid Oxide Electrolysis Cell
SOFC	=	Solid Oxide Fuel Cell
VI	=	Virtual Instrument
YSZ	=	Yttria-Stabilized Zirconia

TEST APARATUS AND STACK INSTALLATION

In 2010, a sixth test station was added to the bench-scale high temperature electrolysis testing capability at the INL. This new test stand added significant additional capability to the lab. At the heart of the test stand is a vertically mounted split tube furnace that provides increased access to the electrolysis test articles without physically removing the furnace. The furnace has an electrical power rating up to 15 kW and can be operated at temperatures up to 1000ºC. It has an inside diameter of 16 inches and a height of 21 inches. The vertical clamshell design provides easy access to the test fixture (inconel 625) that facilitates the supply of process gases and electrical power to

Figure 1. Test stand developed for testing of internally manifolded stacks with electrode-supported cells. Photograph shows the network of remotely controlled motor-operated valves used for steam generation selection.

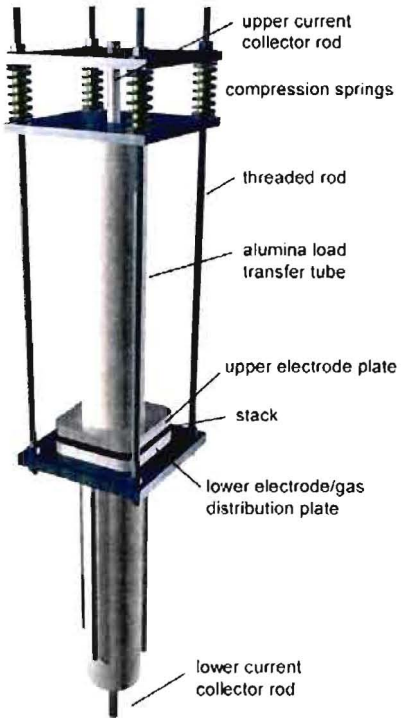

Figure 2. Test fixture detail.

stacks that are on test. A photograph of the furnace, test fixture and supporting instrumentation and valving is provided in Figure 1. The test fixture can be easily adapted to the requirements imposed by a variety of stack configurations.

The test stand includes a choice of three steam delivery systems, allowing a large range of gas flow rates and steam mole fractions to be delivered to the stack on test within the furnace. Steam can be supplied to the test fixture using a traditional humidifer in which a carrier gas mixture is bubbled through a bath of deionized water that is maintained at specified temperature using feedback control. The steam flow rate is determined by the temperature of the water bath and the

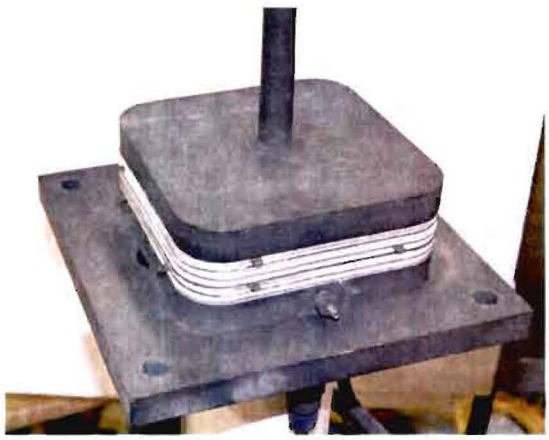

Figure 3. 5-cell MSRI SOEC stack mounted on test fixture.

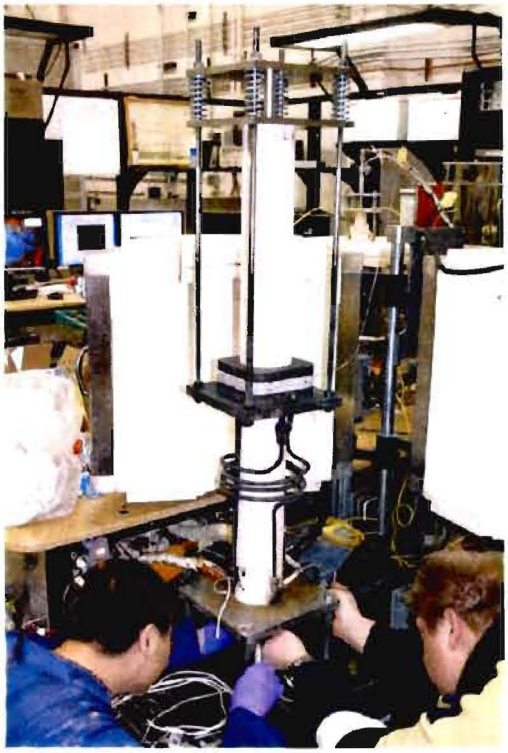

Figure 4. Photograph of a 5-cell MSRI SOEC stack installed in the Test Stand.

flow rate of the carrier gases composed of a controlled mixture of hydrogen and nitrogen. All piping downsteam of the bubbler is heat-traced and insulated to prevent condensation.

The second steam generation method is through the use of a Controlled Evaporator and Mixer (CEM, Bronkhorst). The CEM is built around a liquid mass flow control valve, a gas-liquid mixing device and a heat exchanger in which heat is added to the mixture of fluids for evaporation. De-ionized water and the carrier gas are supplied by separate mass flow controllers. Total evaporation of the water is achieved in the CEM. The piping downstream of the CEM to the furnace is also heat traced and insulated to prevent condensation. There are two complete CEM systems incorporated into the test stand, the smaller of the two has a maximum water flow rate of 100 g/hr and a maximum gas flow rate of 1 slpm with a maximum heater power of 150W. The larger unit can provide up to 1000 g/hr of water and 100 slpm gas flow with a 1kW heater capacity.

The test fixture is based on a design developed at MSRI. It is capable of providing compressive force to the top of a stack while on test through either the addition of dead mass or via compression springs outside of the hot zone of the furnace. When testing stacks produced by MSRI, the compressive load was provided via springs. A total compression load of 181 kg (400 lb) was used. The compression load is transferred to the stack via an alumina tube and the upper electrode plate, as shown in Fig. 2. Once the stack is in place on the lower portion of the test fixture, an alumina load transfer tube is installed atop

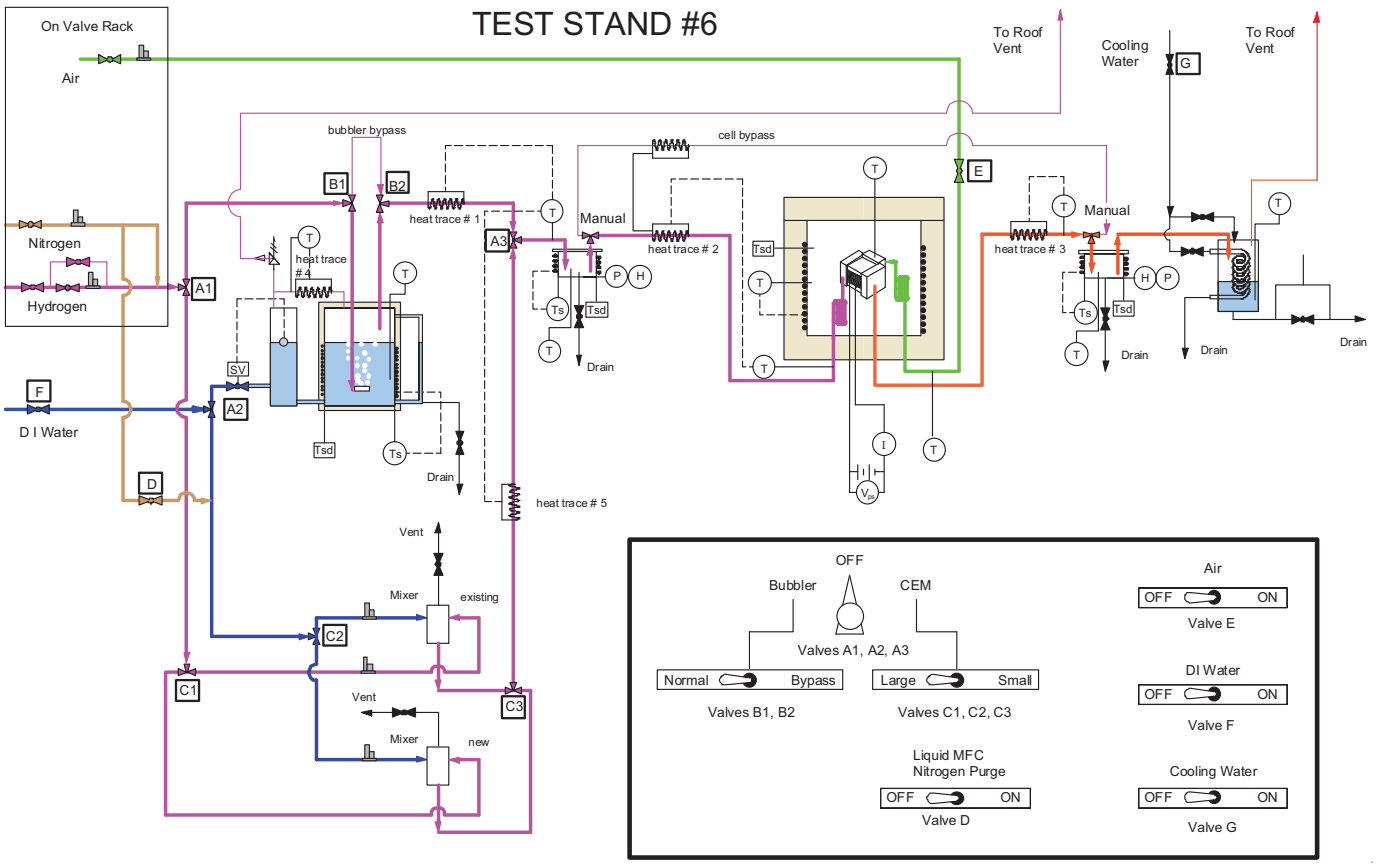

Figure 5: Piping and instrumentation diagram for the INL High Temperature Steam Electrolysis Test Stand 6.

of the upper electrode, onto which compression springs with pusher plates are placed. Compression of the stack to the desired loading is achieved through the tightening of nuts on 4 threaded bars that stand in parallel to the load transfer tube and, fixed to the lower test fixture portion, run through the pusher plates. Upon achieving the desired compression of the springs and hence forced loading of the stack, the furnace may be closed and a heat-up procedure executed. During heat up, the compression of the springs is monitored and carefully adjusted to maintain the prescribed load, and to compensate for thermal expansion of the threaded rods and compression of the compliant seals in the stack. A closeup photograph of the stack mounted on the test fixture is provided in Fig. 3. A photograph of the stack installation in progress is shown in Fig. 4.

A piping and instrumentation diagram (P&ID) for the test stand used for these tests is provided in Fig. 5. Remotely controlled motor-operated valves are used to simplify the selection of the piping configuration for a given desired operating condition. If the humidifier is selected, a bypass option is available to provide dry gas to the stack during startup and cooldown. If the CEM is selected, either the small or large unit is selected. Also a nitrogen purge of the liquid mass flow controllers is available when the CEM option is selected. Three additional valves provide on-off control of the air, DI water and condenser cooling water. Two non-motorized 3-way valves are included in the system to provide a stack bypass option.

Real time test data is collected from in-line instrumentation using a multi-channel data acquisition unit (Agilent) which is interfaced to the system controller computer using a Labview™ based virtual instrument (VI). A programmable DC power supply (lambda™) was used to provide electrical power to a stack while operated in the steam electrolysis mode. A programmable electronic load (Amrel) is used as a power sink for operation of stacks in the fuel cell mode. Switching between the power supply and the electronic load is facilitated by a network of electronic relays housed within a switching box. Both the electronic load and power supply is controlled through the Labview™ VI, allowing for data acquistion and control of DC-potential sweeps for stack performance characterization.

SOLID OXIDE ELECTROLYSIS CELLS AND STACK

The solid oxide cells used for this study have a square profile with outer dimensions of 15.2 cm x 15.2 cm and a cell active area of 100 cm^2. The cells incorporate a negative-electrode-supported multi-layer design with nickel-zirconia cermet negative electrodes, thin-film yttria-stabilized zirconia electrolytes, and multi-layer lanthanum ferrite-based positive electrodes. The nickel zirconia electrode has a support layer

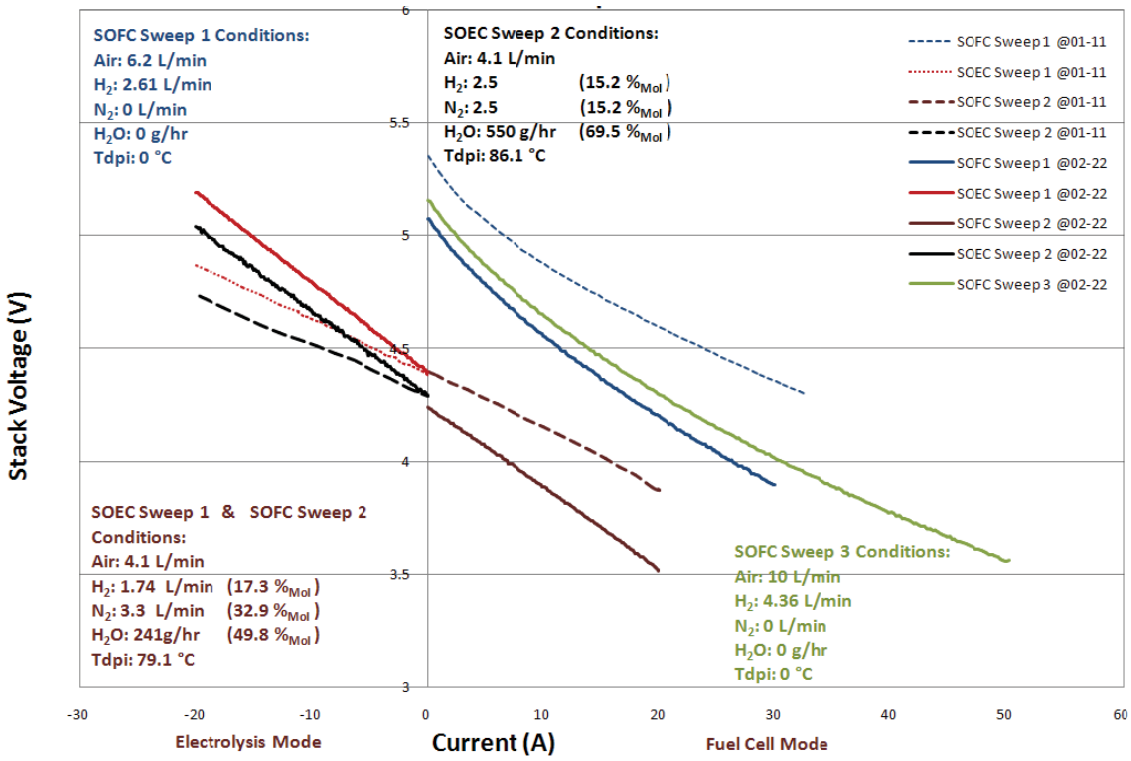

Figure 6: DC-Potential SOEC and SOFC polarization curves for the MSRI stack tested at INL. Final results were obtained after 1000 hours of operation in the steam electrolysis mode with a current density of 0.2 A/cm^2.

thickness of 700 µm and a graded functional layer with an overall thickness of 15 µm. The electrolyte thickness is 8 – 10 µm. The positive electrode also has a graded functional layer with a thickness of 20 µm and the current collecting layer thickness is 50 µm.

The stack is internally manifolded with compliant seals. Treated metallic interconnects with integral flow channels separate the cells and electrode gases. The cells incorporate semi-elliptical cutout gas flow channels, four per side around the outer periphery of the cells, that mate with corresponding holes in the interconnect plates and compliant seals. The stack operates in cross-flow, with an inverted-U shaped overall flow pattern such that the gas flow inlets and outlets are all located underneath the stack. Stack mechanical compression is accomplished by means of the custom spring-loaded test fixture described previously.

Installation of MSRI stacks within the test section is a relatively simple procedure. Correct alignment of the process gas (steam/H_2) and air inlets and outlets of the stack to the corresponding flow channels of the test section is most critical. Compliant gasket seals are placed underneath and atop of the stack prior to placement on the test fixture lower electrode / gas distribution plate. Contact aids are used to assist electrical contact between the stack and the upper and lower fixture electrodes.

RESULTS - INL TESTS

A 5-cell MSRI stack was installed in the INL High Temperature Steam Electrolysis Laboratory's test stand number 6 On the 10th of January 2011. The stack was maintained at a temperature of 800°C after controlled heat-up, seal curing, and a cell reduction procedure (with a dry forming gas) were completed. Table 1 summarizes the heat-up procedure used for the MSRI 5-cell stack.

Once the seals were cured and the cells of the stack were fully reduced a stable open cell voltage (OCV) was achieved. Initial characterization of the cells and overall stack performance was determined through a series of DC-potential (V-I) sweeps obtained over a range of inlet conditions in both fuel cell and electrolysis modes of operation. Approximate inlet conditions of 0 %$_{Mol}$, 50 %$_{Mol}$ and 70%$_{Mol}$ steam were examined for the influence of steam on the stack performance. These molar concentrations may be considered in terms of inlet dew point temperatures of 0, 79.1 and 86.1°C, respectively. Upon completion of initial characterization, the stack was placed into long-term SOEC testing for 1000 hours operation with a current density of 0.2 A/cm^2 (20 A total current) and inlet dew point value of 86.1 °C. After 1000 hours of testing, a final set of DC-potential sweeps were recorded.

Fig. 6 illustrates a comparison of the initial V-I sweep data recorded on the 11th January 2011 to the final sweeps after 1000 hours of testing in the electrolysis mode recorded on the 22nd of February 2011. SOFC sweep 1, 1-11 was performed with only

Table 1: Summary of the MSRI Stack heat-up procedure and operating conditions.

Step	*Temperature (°C)*	*Compressive load (Lb)*	*H_2 Flow (SLPM)*	*N_2 Flow (SLPM)*	*Airside Flow (SLPM)*
1	0 → 600 @ 5 °C/min	100	0.45	4.05	4.5 - N_2
2	600 → 830 @ 5 °C/min	400	0.45	4.05	4.5 - N_2
3	830 0.5 hour hold	400	0.45	4.05	4.5 - N_2
4	830 → 800 @ 5 °C/min	400	0.45	4.05	4.5 - N_2
4	800 1 hour hold	400	0.45	4.05	4.5 - N_2
4	800 1 hour hold	400	1.2	4.8	6.0 - N_2
5	800 1 hour hold	400	1.8	4.2	6.0 - N_2
6	800 Long Term Operation	400	2.5	2.5	4.1 – N_2

dry hydrogen flowing on the fuel side. The VI curve for this sweep exhibits significant curvature at low current density. This effect is associated with the high sensitivity of the Nernst potential to small changes in average steam concentration as cells begin to convert hydrogen to steam in the fuel cell mode. SOFC sweep 2, 1-11, and SOEC sweep 1, 1-11 were performed with 50% mole fraction steam. These sweeps exhibit nearly linear behavior that is continuous in the fuel cell and electrolysis modes. SOEC sweep 2, 1-11, was performed with 70% steam. Note that the open-cell (zero-current) potential decreases with higher steam content. This sweep shows nearly linear VI behavior with a slop that is parallel to SOEC sweep 1, 1-11.

Final VI sweeps were obtained after 1000 hours of operation in the SOEC mode. In all cases, the final sweeps have slightly steeper slopes than the corresponding initial sweeps, as expected, due to performance degradation.

Results from the 1000-hour INL test are presented in Figs. 7 - 9. Fig. 7 shows the overall stack voltage and current for the 1000-hr test. The test was performed at a constant current of 20 A. Stack voltage increased from 4.58 V to 5.047 V over the test duration, indicating a degradation rate of 10.2%/khr based on voltage. An expanded view of the stack voltage is presented in Fig. 8 along with the inlet and outlet dewpoint values. The outlet dewpoint values are ~3.5°C lower than the inlet values, which is consistent with the electrolytic conversion of steam to hydrogen at these gas flow rates and at this amperage. The dewpoint measurements allow for independent determination of the steam consumption/hydrogen production rate. This figure indicates fluctuations in stack voltage that correlate with fluctuations in dewpoint values observed during the first 800 hours of the test. These fluctuations were attributed to significant drops in facility water

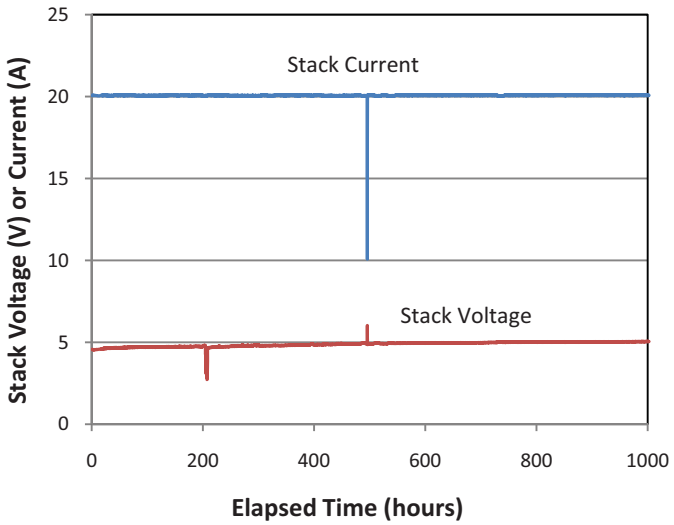

Figure 7. Stack voltage and current, long-term test.

pressure that resulted in the reduction in steam production. These fluctuations in water pressure were rectified at approximately 800 hours into the test through the installation of a booster pump downstream of the mains water supply, ahead of the water purification system.

Another notable artifact of a significant test anomaly is evident in Figures 6 and 7 at approximately 210 hours when the gas generator partially failed to operate on a liquid nitrogen dewar used to supply nitrogen gas to the test facility. The reduction in nitrogen gas supply resulted in increased steam molar concentrations and hence a dramatic drop in SOEC operating voltage. This problem was rectified rapidly by the switching of the nitrogen gas supply to a secondary nitrogen dewar.

Individual cell voltages recorded during the long-term test are presented in Fig. 9 along with the apparent area-specific resistance (ASR) values (stack operating voltage minus stack

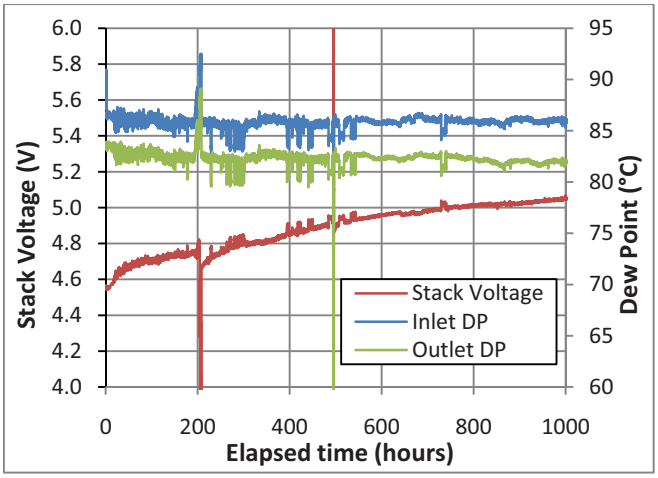

Figure 8: Stack voltage and dewpoint temperatures, 1000-hr INL test.

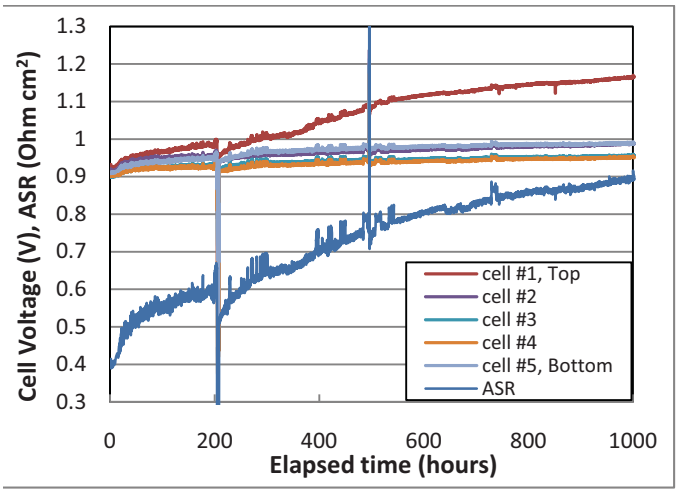

Figure 9. Individual cell voltages, long-term test, current density of 0.2 A/cm^2 and an inlet steam molar concentration of 69.5 %$_{Mol}$. The apparent stack ASR and its behavior as a function of time is also indicated.

open-cell voltage divided by current density). The individual cell voltages are very steady, with the exception of the top cell, which increases dramatically during the long-term test. In fact, cell 1 degraded at a rate of approximately 24.1 % per 1000 hours while cell 4 (the second from the bottom of the stack) exhibited the lowest degradation rate of only 3.28 % per 1000 hours. Clearly the overall degradation of the stack was significantly influenced by the degradation of the uppermost cell. We are investigating the possible causes of the accelerated degradation of that cell. The initial stack ASR value was 0.41 Ωcm^2. The stack ASR increased to 0.89 by the end of the 1000-hr test.

RESULTS - MSRI TESTS

As mentioned previously, an identical companion 5-cell

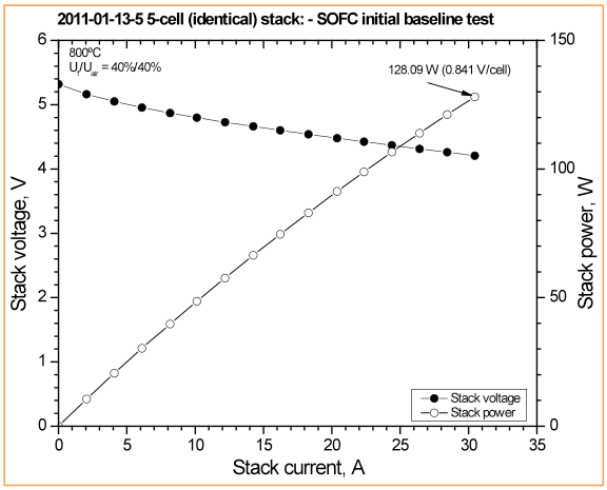

Figure 10. Initial stack voltage and power, 5-cell stack tested at MSRI. Hydrogen and air utilization set at 40%

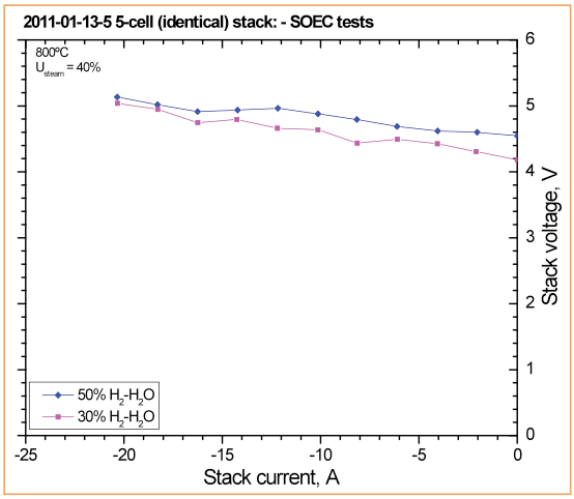

Figure 11. Initial SOEC sweep, MSRI test, steam utilization fixed at 40%.

stack was tested at MSRI in a similar test stand and with similar operating conditions. Results of an initial sweep performed in the fuel cell mode are presented in Fig. 10. This sweep was performed in a stepwise fashion, allowing for adjustments of hydrogen and air flow rates such that both the fuel and air utilizations were fixed at 40%. As shown in the figure, at 30.4 amps, the stack generated 128.09 W of electrical power at 4.205 V (or 0.841 V/cell). After the SOFC baseline test, the same stack was evaluated in the SOEC mode with the steam utilization fixed at 40%. Results are shown in Fig. 11. The concentrations of steam carried by H_2 on the negative electrode varied from 50% to 70%. At 20.3 amps, the stack respectively consumed 104.48 W and 102.44 W of power for steam concentrations of 50% and 70% bal. H_2 in the electrolysis mode.

Results of the long-term 1100-hr durability test performed at MSRI are presented in Fig. 12. The test was performed at a

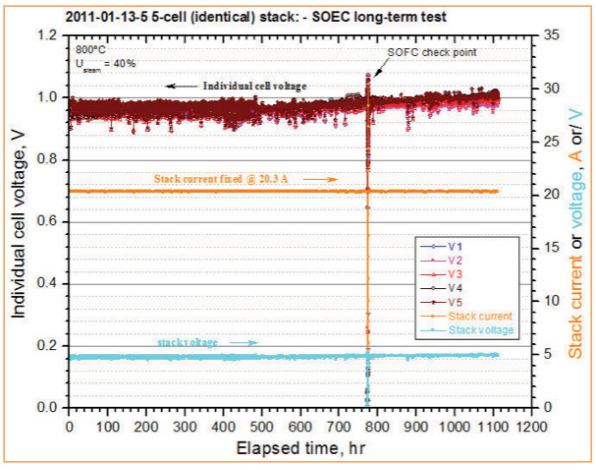

Figure 12. Results of long-term 1000-hr SOEC durability test performed at MSRI.

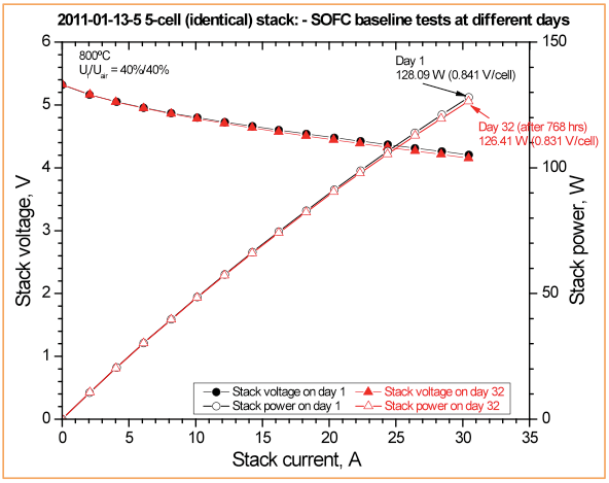

Figure 13. Comparison of final and initial sweeps, MSRI test, SOFC mode.

fixed current of 20.3 A with a fixed steam utilization of 40%. This stack demonstrated a degradation rate of less than 3%/khr, based on voltage. This low degradation rate is remarkable and it represents significant progress toward a commercial viability. On day 32 (after 768 hours continuous test), the long-term test was interrupted for a scheduled operation in SOFC mode (power generation mode) which serves as a check-point for the stack functionality. The results of this sweep are presented in Fig. 13. Comparison of the initial and day 32 sweeps confirms that degradation was minimal.

SUMMARY AND CONCLUSIONS

Results of performance characterization and durability testing have been presented for two five-cell high-temperature electrolysis stacks constructed with advanced electrode-supported cells and internally manifolded stack technologies. One stack was tested at the Idaho National Laboratory and an identical stack was tested at MSRI. A detailed description of a new test station at INL was provided. Test results indicated excellent initial performance and low overall degradation rates. The overall degradation rate for the INL stack was 10.2%/khr, but degradation for this stack was dominated by one cell that exhibited a very high degradation rate of 24.1%/khr. The overall degradation rate for the MSRI-tested stack was less than 3%/khr. This low degradation rate is remarkable for the SOEC mode of operation.

ACKNOWLEDGMENTS

This work was supported by the U.S. Department of Energy, Office of Nuclear Energy, Next Generation Nuclear Plant Program under DOE Operations Office Contract DE-AC07-05ID14517.

REFERENCES

1. Forsberg, C. W., "The Hydrogen Economy is Coming. The Question is Where?" *Chemical Eng. Progress*, Dec. 2005, pp. 20-22.
2. Lewis, D., "Hydrogen and its relationship with nuclear energy," *Progress in Nuclear Energy*, Vol. 50, pp. 394-401, 2008.
3. Kruger, P., "Nuclear Production of Hydrogen as an Appropriate Technology," *Nuclear Technology*, Vol. 166, pp. 11-17, 2009.
4. Forsberg, C. W., "Future hydrogen markets for large-scale hydrogen production systems," *Int. J. Hydrogen Energy*, Vol. 32, pp. 431-439, 2007.
5. Duffey, R. B., "Nuclear production of hydrogen: When worlds collide," *International Journal of Energy Research*," Vol. 33, pp. 126-134, 2009.
6. Granovskii, M., Dincer, I., and Rosen, M. A., "Greenhouse gas emissions reduction by use of wind and solar energies for hydrogen and electricity production: economic factors," *Int. J. Hydrogen Energy*, V. 32, 2007, pp. 927-931.
7. Rand, D. A. J., and Dell, R. M., *Hydrogen Energy: Challenges and Prospects*, Royal Society of Chemistry, 2008.
8. Floch, P-H., Gabriel, S., Mansilla, C., and Werkoff, F., "On the production of hydrogen via alkaline electrolysis during off-peak periods," *Int. J. Hydrogen Energy*, Vol. 32, 2007, pp. 4641-4647.
9. Schultz, K. R., Brown, L. C., Besenbruch, G. E. and Hamilton, C. J., "Large-Scale Production of Hydrogen by Nuclear Energy for the Hydrogen Economy," Report GA-A24265, Feb. 2003, 22p.
10. O'Brien, J. E., Stoots, C. M., Herring, J. S., and Hartvigsen, J. J., "Performance of Planar High-Temperature Electrolysis Stacks for Hydrogen Production from Nuclear Energy," *Nuclear Technology*, Vol. 158, pp. 118 - 131, May, 2007.
11. Steinfeld, A. "Solar thermochemical production of hydrogen," *Solar Energy*, V 78, No 5, pp. 603-615, May 2005.
12. Southworth, F., Macdonald, P. E., Harrell, D. J., Park, C. V., Shaber, E. L., Holbrook, M. R., and Petti, D. A., "The Next Generation Nuclear Plant (NGNP) Project," Proceedings, Global 2003, pp. 276-287, 2003.
13. Schultz, K., Sink, Pickard, P., Herring, J. S., O'Brien, J. E., Buckingham, R., Summers, W., and Michele Lewis, M., "Status of the US Nuclear Hydrogen Initiative," Proceedings of ICAPP 2007, Paper 7530, Nice, France, May 13-18, 2007; *The Nuclear Renaissance at Work*, V. 5, Societe Francaise d'Energie Nucleaire – ICAPP 2007, pp. 2932-2940.
14. Stoots, C. M., O'Brien, J. E., Condie, K., Moore-McAteer, L., Housley, G. K., Hartvigsen, J. J., and Herring, J. S., "The High-Temperature Electrolysis Integrated Laboratory Experiment," *Nuclear Technology*, April, 2009.
15. Varrin, R. D., Reifsneider, K., Scott, D. S., Irving, P., and Rolfson, G., "NGNP Hydrogen Technology Down-Selection; Results of the Independent Review Team Evaluation," Dominion Engineering report# R-6917-00-01, August, 2009.

16. Hauch, A. (2007). "Solid Oxide Electrolysis Cells – Performance and Durability," Ph.D. Thesis, Technical University of Denmark, Risø National Laboratory, Roskilde, Denmark.
17. Tanasini, P., Cannarozzo, M., Costamagna, P., Faes, A., Van Herle, J., Hessler-Wyser, A., and Comninellis, C., "Experimental and theoretical investigation of degradation mechanisms by particle coarsening in sofc electrodes," *Fuel Cells*, v 9, n 5, p 740-752, October 2009.
18. Butz, B., Kruse, P., Stormer, H., Gerthsen, D., Muller, A., Wever, A., and Ivers-Tiffee, E., "Correlation between Microstructure and Degradation in Conductivity for Cubic Y2O3-doped ZrO2," Solid State Ionics, Vol. 177, Issue 37, pp. 3275-3284, 2006.
19. Marina, O. A., Pederson, L. R., Williams, M. C., Coffey, G. W., Meinhardt, K. D., Nguyen, C. D., and Thomsen, E. C., "Electrode Performance in Reversible Solid Oxide Fuel Cells, J. Electrochemical Soc., Vol. 154, No. 5, pp. B452-B459, 2007.
20. Svensson, A. M., Sunde, S., and Nisancioglu, K, "Mathematical Modeling of Oxygen Exchange and Transport in Air-Perovskite-Yttria-Stabilized Zirconia Interface Regions," J. Electrochemical Soc., Vol. 145, No. 4, pp. 1390-1400, April 1998.
21. Virkar, A. V., "Mechanism of Oxygen Electrode Delamination in Solid Oxide Electrolyzer Cells," Int. J. Hydrogen Energy, in review, 2010.